





Multidimensional Response Evaluation of Remote-Sensing Vegetation Change to Drought Stress in the Three-River Headwaters, China

Shuang Zhu , Zuxiang Xiao , Xiangang Luo , Hairong Zhang, Xiuwei Liu, Rui Wang, Mingzhi Zhang , and Zhibin Huo

Abstract—The impact of drought on ecosystems has become increasingly prominent. This study used the MODIS remote-sensing vegetation index and the standardized precipitation index to quantify vegetation coverage status and meteorological drought level. Using the copula method, the joint distribution of the drought index and related vegetation cover variables were simulated for the first time. The conditional distribution of vegetation biomass was deduced, and the multidimensional response between the vegetation biomass and drought was explored to understand the possible vegetation loss under different drought severity conditions. The three-river headwaters (TRH) region is the source place of the Yangtze River, Yellow River, and Lancang River, where the ecosystem is characterized by the innate vulnerability. Using this region as a case study, the results show that the spatiotemporal evolution of drought and vegetation in the TRH region has apparent regional heterogeneity. The vegetation cover in the eastern region is significantly better than that in the northwestern region, while the vegetation growth trend in the northwestern region is stronger than that in the southeastern region. It is feasible to build a vegetation-drought multidimensional response model based on the copula method. In 92.5% of the TRH region, vegetation cover was significantly affected by the severity of the drought. The impact on the growth of vegetation caused by persistent drought events was higher than that of short-term but high-intensity drought. The vegetation in the TRH area has a certain degree of drought resistance. This study provides outstanding theoretical support and reference for the protection of the TRH basin ecosystem.

Index Terms—Copula method, meteorological drought, multidimensional response, remote-sensing vegetation, three-river headwaters (TRH).

I. INTRODUCTION

DROUGHT refers to a phenomenon that has a wide range of negative effects on ecosystems, agricultural production, the water environment, and human activities and is defined as a period when the amount of available water is well below the long-term recorded averages. Among the various natural and human communities affected, the degraded terrestrial ecosystems that have suffered severe drought stress may subsequently trigger a series of surface and atmospheric responses [1], [2]. Continuous meteorological and hydrological droughts will affect vegetation growth in ecosystems. In recent years, the response of ecosystems to drought events has become a popular research issue [3]. In addition to global warming, drought events frequently occur throughout the world, causing severe ecological and environmental impacts [3]. Guttman [4] proposed the Palmer drought severity index for assessing the severity of meteorological drought. McKee *et al.* [5], [6] proposed the standardized precipitation index (SPI), which has an excellent performance in studies on the temporal and spatial characteristics of drought [7]. Vegetation cover is an essential factor that reflects the ecological environmental change. For the long-term vegetation change monitoring, satellite remote-sensing data sources, such as the normalized difference vegetation index (NDVI) and the enhanced vegetation index (EVI), can usually be used [8]. The NDVI is widely used for measuring vegetation cover [9]. The EVI has the advantage of relatively high spatial and large-area near-real-time data resolution [10].

The impact of drought on pasture growth and Yellow River water is inestimable. Studies have confirmed that the response of vegetation biomass to drought degree can be used to better assess the different levels of drought resistance between various ecosystems. Moreover, this information is valuable and provides essential theoretical support and reference for protecting the ecosystem [11]–[13]. There are many studies currently addressing vegetation response to precipitation or temperature changes at regional and global scales, and these studies aim to clarify the main driving factors of the evolution of stressed ecosystems [14]–[16]. Scholars usually use the correlation coefficient or partial correlation coefficient method to determine the

Manuscript received May 18, 2020; revised August 9, 2020 and September 16, 2020; accepted September 21, 2020. Date of publication September 29, 2020; date of current version October 23, 2020. This work was supported by the National Natural Science Foundation of China under Grant 51809242 and Grant 51909010. (Corresponding authors: Xiangang Luo; Mingzhi Zhang.)

Shuang Zhu, Zuxiang Xiao, and Xiangang Luo are with the School of Geography and Information Engineering, China University of Geosciences, Wuhan 430074, China, and also with the National Engineering Research Center for Geographic Information System, China University of Geosciences, Wuhan 430074, China (e-mail: zhushuang@cug.edu.cn; giserxxz@cug.edu.cn; luoxiangang@cug.edu.cn).

Hairong Zhang is with the Water Resources Center, China Yangtze Power, Company, Ltd., Yichang 443133, China, and also with the Water Resources Center, Hubei Key Laboratory of Intelligent Yangtze and Hydroelectric Science, Yichang 443133, China (e-mail: zhang_hairong@ctg.com.cn).

Xiuwei Liu and Rui Wang are with the Geological Hazard Technical Service Center of Guizhou Province, Guiyang 550001, China (e-mail: liuxiuwei@gmail.com; wangrui@gmail.com).

Mingzhi Zhang is with the Institute of Geological Environment Monitoring, China Geological Survey, Beijing 100081, China (e-mail: zhangmingzhi@gmail.com).

Zhibin Huo is with the Institute of Hydrogeology and Environmental Geology, Chinese Academy of Geological Sciences, Hebei 050061, China (e-mail: huozhibin@gmail.com).

Digital Object Identifier 10.1109/JSTARS.2020.3027347

simple linear relationship between the meteorological drought and vegetation index on different time scales and lag periods [17]. Studying the correlation between the vegetation index and climate variables, Dutta *et al.* [18] used the SPI meteorological drought index to feedback the vegetation condition index (VCI). Scholars calculated that there was a strong positive correlation between the VCI and rainy season crop yield, which verified that the VCI estimation could be used to monitor the occurrence and development of agricultural drought [19]–[21]. Cassim and Juma [22] used the correlation between the VCI and varying degrees of drought SPI values to more thoroughly analyze the intensity changes of drought events. Nanzad *et al.* [23] examined the Pearson correlation between the climatic variables and NDVI abnormalities and concluded that the NDVI abnormalities were positively correlated with seasonal precipitation anomalies for 17 years.

Currently, temperature and precipitation are the most representative variables used in research on the correlation between vegetation and climate change [24]. Chen and Yongming [25] also noted that the NDVI value in the MODIS vegetation index is higher than the EVI value and both have a high correlation. Additionally, Ji and Peters [26] showed that the three-month SPI had the highest relationship with the NDVI, and Haro-Monteagudo *et al.* [27] reported that the drought index at the three-month time scale had the highest correlation with vegetation change. The linear correlation between the vegetation indices and climatic factors is considered suitable for studying the response of vegetation to drought [28], [29]. However, drought has a sizeable negative impact on ecosystems. Drought slows vegetation growth, reduces the green degree, decreases biomass per unit area, and even causes vegetation death [30]. The different physiological responses of vegetation under drought conditions determine the resistance to water growth and resilience. The simple correlation analysis cannot fully reveal the depth and breadth of vegetation change responses [31]–[33]. Thus, a thorough understanding of the response of vegetation to drought has become particularly important.

The copula function connects the joint distribution function with its marginal distribution function. It can simulate the multivariate joint distribution between the random variables and model its secondary structure [34]. The copula function can flexibly choose any margin, which facilitates the expansion of two variables and allows the analysis of the marginal distribution and dependence structure between the multiple variables. Early copula theory is widely used abroad in the study of financial risk and insurance [35]. Today, it has been successfully used for the multivariate analysis of hydrological drought, including the severity, intensity, and duration of drought [36]–[38]. Xu *et al.* [39] studied the temporal and spatial variation characteristics of drought in southwestern China through copula frequency analysis. Fang *et al.* [40] used the copula method to establish a joint probability model of drought index and vegetation change and obtained a strip response to the vegetation index under specific drought conditions. The copula function is widely used in the multivariable edge distribution function of different feature variables in multiple research fields to fit the joint distribution. According to the author's knowledge, this research method is

rarely used in research areas related to agricultural drought disasters. When a drought event occurs, it will affect the healthy growth of crops to a certain extent [41]. Fang *et al.* [40] built a binary probability model based on the copula function to assess the vulnerability of vegetation in the Loess Plateau of China. The study constructed a joint distribution of SPI and NDVI sequences but did not discuss the SPI extremes and NDVI loss at the beginning and end of drought events in depth, and these processes are more closely related to the ecological environment. At the same time, except for the NDVI, studies about EVI indicators with high data representativeness are scarce. Using the copula function to construct the dependence of vegetation coverage to different drought characteristics can improve the regional ability to address meteorological drought and promote the sustainable development of vegetation and agriculture in arid regions.

The three-river headwaters (TRH) region is the source catchment area of the Yangtze River, Yellow River, and Lancang River. It is a sensitive area and a fragile zone in international scientific and technological circles and has been used to study the climate and ecological environmental changes [42]. Vegetation cover, climate change, and environmental protection in this area have been the focus of research [43], [44]. In recent decades, the TRH area has shown trends of increased temperature, reduced precipitation, and increased evaporation [45]. This change has not only caused environmental degradation but also indirectly threatened water resource security in the middle and lower reaches of the three rivers [46]. Here, combining the drought indicator SPI and remote-sensing vegetation index (NDVI/EVI), this article profoundly quantifies the multiple vegetation-drought responses in the TRH region by introducing the copula method. The research objectives of this article are as follows: First, to analyze the multiscale spatiotemporal characteristics of drought and vegetation cover, and second to develop a conditional copula method to evaluate the multiple responses of vegetation growth to drought climate conditions. The remainder of this article is organized as follows. The study area and datasets are described in Section II. The methods are explained in Section III. Section IV presents the results. Section V discusses the research focus of this article and compares the previous study. Section VI concludes the article with a summary.

II. STUDY AREA AND DATASETS

A. Study Area

The TRH region is located in the southern part of Qinghai Province, China, with an area of approximately 363 000 km². The Yangtze River, the Yellow River, and the Lancang River originate in this region, and it is also the hinterland of the Qinghai–Tibet Plateau (see Fig. 1). In Fig. 1, the watersheds are divided into red, yellow, and jade green to represent the Yangtze River, the Yellow River, and the Lancang River, respectively. The gray part is the internal area where the river disappears or flows into the inland lake. The annual average runoff of the THR from the Yellow River, the Yangtze River, and the Lancang River is 20.1 m³, 12.4 m³, and 15.0 × 10⁹ m³, respectively. The

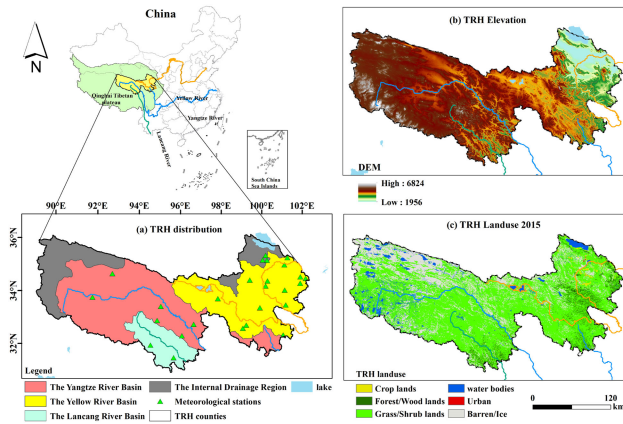


Fig. 1. Location of the TRH region and its subregions, DEM, and land-use type in 2015.

area is located in the temperate zone. The annual precipitation is 262–773 mm, and the annual evaporation is between 730 and 1700 mm. More than 80% of the annual precipitation occurs from May to October [47]. A total of 20 national meteorological stations are located in the study area and shown in Fig. 1(a). The digital elevation model of the TRH region is shown in Fig. 1(b). Fig. 1(c) shows the land-use types in 2015, which are mainly forestland and grassland, and vegetation is the most important land-use type in the area.

B. Data Sources and Processing

The digital elevation model in this study came from the geospatial data cloud website.¹ The land-use coverage data of the Qinghai-Tibet Plateau came from the Resource and Environmental Science Data Center of the Chinese Academy of Sciences,² and the land-use types in the TRH region were obtained through cutting and reclassification. The remote-sensing satellite data MOD13Q1 came from the National Aeronautics and Space Administration EOS/MODIS data product³ with a spatial resolution of 250×250 m and a temporal resolution of 16 d. The MOD13Q1 vegetation index products (NDVI and EVI) are treated with water, clouds, and heavy aerosols. The two products adequately characterize the global vegetation status and processes and are widely used in regional vegetation cover change studies to ensure the data quality. In this article, remote-sensing data were reprojected and roughly cropped using the MODIS reprojection tool. The maximum value composite was used to synthesize monthly NDVI data to eliminate the influence of outliers, and the monthly NDVI data were integrated into the most significant annual NDVI image [42]. We processed the remote-sensing vegetation index (NDVI/EVI) from 2000 to 2018. For a more detailed drought assessment, this article uses the monthly ground precipitation data from 40 meteorological stations in the TRH region. The data came from the China meteorological science data sharing service network.⁴ The time

TABLE I
DROUGHT SEVERITY CLASSIFICATION IN CHINA

Grade	Category	SPI Value	Probability (%)
I	Wet	$SPI > -0.50$	50.0
II	Mild drought	$-1 < SPI \leq -0.50$	34.1
III	Moderate drought	$-1.5 < SPI \leq -1.00$	9.2
IV	Severe drought	$-2 < SPI \leq -1.50$	4.4
V	Extreme drought	$SPI \geq -2.00$	2.3

span is from 1961 to 2018. The data were cross validated, analyzed for error, and of good quality.

III. METHODOLOGY

A copula joint distribution model is constructed for studying multiple nonlinear responses of drought conditions and vegetation variation. Specifically, the copula model is introduced to develop the dependent structure of drought conditions and vegetation growth series. The marginal distribution of each concerned variable is fit with the appropriate single-variable distribution. The response analysis based on the copula method is derived from the conditional joint distribution. Related theories and methods are described in the following sections.

A. Meteorological Drought Index

The SPI [5] is one of the most commonly used meteorological drought indices. It can be calculated at multiple time scales, and it assumes that the precipitation is subject to the gamma distribution, taking into account the reality of the precipitation obeying the skewed distribution. When the SPI value is continuously observed to be less than or equal to 0, it is defined as a drought event [5], [48]. A detailed description and computer program for the specific SPI can be obtained from the National Drought Mitigation Center website.⁵ The SPI has substantial flexibility. The selection of the vegetation growing season makes it conducive to understand agricultural drought [49]. Table I lists the drought classification criteria in China.

B. Vegetation Status Index

The NDVI is the most widely used vegetation index. It reflects the coverage of vegetation and the necessary growth state of vegetation. The EVI is an enhanced vegetation index that improves factors, such as atmospheric noise, soil background, and saturation. Compared with the NDVI, the EVI is less commonly used for vegetation and climate response studies [25]. The vegetation growing season in the TRH area is from May to September every year when the vegetation begins to appear as bright green. The impact of drought on vegetation growth mainly occurs in the vegetation growing season. Therefore, the NDVI and EVI from May to September of each year were extracted for vegetation spatiotemporal feature analysis and response analysis.

¹[Online]. Available: <http://www.gscloud.cn/>

²[Online]. Available: <http://www.resdc.cn/>

³[Online]. Available: <https://modis.gsfc.nasa.gov/>

⁴[Online]. Available: <http://cdc.cma.gov.cn/>

⁵[Online]. Available: <http://www.drought.unl.edu/monitor>

C. Mann–Kendall (MK) Trend Test

The MK nonparametric test [50], [51] is frequently used to evaluate trends in time series of precipitation, runoff, temperature, etc. It has the advantage that the sample does not need to follow a specific distribution. In addition, it is unaffected by outliers.

Suppose there is a time series of sample size n (x_1, \dots, x_n); for all $k, j \leq n$ and $k \neq j$. The distributions of x_k and x_j are different, and the test statistic is calculated as follows:

$$S = \sum_{k=1}^{n-1} \sum_{j=k+1}^n \text{Sgn}(x_j - x_k) \quad (1)$$

where Sgn is the signum function

$$\text{Sgn}(x_j - x_k) = \begin{cases} 1(x_j - x_k) > 0 \\ 0(x_j - x_k) = 0 \\ -1(x_j - x_k) < 0 \end{cases} \quad (2)$$

In the formula, S is a normal distribution with a mean of 0, and the variance is $\text{var}(S) = n(n-1)(2n+5)/18$. When $n > 10$, the standard normal statistical variables are calculated by the following:

$$Z = \begin{cases} \frac{S-1}{\sqrt{\text{Var}(S)}}, & S > 0 \\ \frac{S+1}{\sqrt{\text{Var}(S)}}, & S < 0 \end{cases} \quad (3)$$

When the value is greater than 0, it represents an increasing trend; in contrast, when the value is less than 0, it represents a decreasing trend. When the absolute values are higher than 1.28, 1.64, and 2.32, the significance tests of 90%, 95%, and 99% confidence are passed, respectively. Moreover, to reduce the influence of the dependent time series on the trend, Hurst index, cycle, etc., the prewhitened method was used to eliminate the correlation. We used MATLAB statistical software to write a cyclic calculation program for MK trend analysis to obtain the values for all sites.

D. Drought Conditions and Vegetation Growth

To explore the response of vegetation variation to drought conditions, several extra variables need to be constructed based on the original SPI and NDVI/EVI series. For drought conditions, the minimum SPI3 value (labeled MIN_SPI) in the growing season of each year is extracted to represent the drought intensity peak, and the accumulated negative SPI3 value (labeled AN_SPI) in the growing season of each year is extracted to represent the drought severity. The NDVI/EVI difference between the beginning of the growing season and the end of the growing season is defined as the vegetation variation value (labeled Var_NDVI/Var_EVI).

To explore the response degree of the vegetation index to different drought conditions more deeply, the quantiles of 0.05/0.25/0.5/0.75/0.95 in the conditional NDVI/EVI distribution were derived. They were defined as q_NDVI/q_EVI. For drought conditions, the average SPI1 in the growing season was extracted to indicate the severity of the drought.

E. Copula Joint Distribution Function

The copula function has the advantages of flexibility, multivariate, and independence, and it is an effective way to establish a joint distribution. It considers two random variables, X and Y , and a connection function, C . The following equation is derived as [52]:

$$F_{X,Y}(x, y) = C(F_X(x), F_Y(y)). \quad (4)$$

The $F_{X,Y}(x, y)$ function defines a 2-D distribution function with marginal distribution $F_X(x)$ and $F_Y(y)$. If $F_X(x)$ and $F_Y(y)$ are continuous, there is only one copula function. Then, the joint density distribution function is as follows:

$$f_{X,Y}(x, y) = c(F_X(x), F_Y(y))F_X(x)F_Y(y) \quad (5)$$

where C is the copula density function

$$C(u, v) = \frac{\partial^2 C(u, v)}{\partial u \partial v} \quad (6)$$

where $u = F_X(x)$ and $v = F_Y(y)$.

For a marginal distribution, a Gaussian distribution is used for modeling vegetation variation (Var_NDVI/Var_EVI). The generalized extreme value (GEV) model is suitable for the drought condition variables of MIN_SPI/AN_SPI, which represents a climate extreme event. (7) is the formula for GEV [53]. Using the standardized variable $s = (x - \mu)/\sigma$, the cumulative distribution function of the GEV distribution is as follows:

$$F(s; \xi) = \begin{cases} \exp(-(1 + \xi s)^{-1/\xi}) & \xi \neq 0 \\ \exp(-\exp(-s)) & \xi = 0 \end{cases} \quad (7)$$

where $\mu \in \mathbb{R}$ is the location parameter, σ is the scale parameter and $\sigma > 0$, and $\xi \in \mathbb{R}$ is the shape parameter.

This article uses the Kendall correlation coefficient to evaluate the correlation between the characteristic variables of the joint distribution model. The Kendall correlation coefficient is a statistical value used to measure the correlation between two random variables and is usually represented by the Greek letter τ (tau). The value of tau ranges from -1 to 1 . A strong correlation exists between two random variables if the absolute value of tau equals 1. The sign of tau represents a positive or negative correlation. These two random variables are independent of each other if tau equals 0 [54]. For the goodness-of-fit test statistic, the associated p values were calculated using the bootstrap method. A very low p value (< 0.05) signified that the null hypothesis that the copula function was a valid model should be rejected. When the p value is larger, the validity of the model is more significant [55].

F. Response of Vegetation to Drought Conditions

Suppose x represents the variable MIN_SPI/AN_SPI/SPI1, y represents the variable Var_NDVI/Var_EVI/q_NDVI, and the copula joint distribution of x and y is $F_{x,y}(x, y)$. The marginal distribution of x is $F_x(x)$ and that of y is $F_y(y)$. The vegetation response under different drought categories is derived as follows:

For MIN_SPI, if $-1 < x \leq -0.50$, mild drought is detected. Then, the conditional distribution of vegetation variation is as

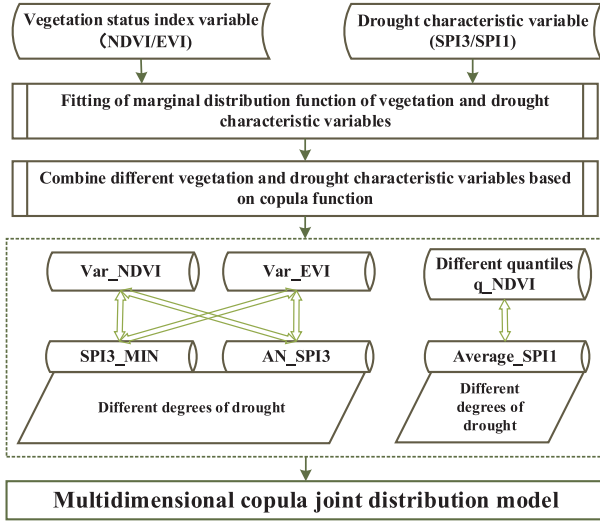


Fig. 2. Flowchart of the multidimensional copula joint distribution model.

follows:

$$\begin{aligned}
 P(y | -1 < x < -0.5) &= \frac{P(y, -1 < x < -0.5)}{P(-1 < x < -0.5)} \\
 &= \frac{P(y, x < -0.5) - P(y, x < -1)}{P(-1 < x < -0.5)} \\
 &= \frac{F_{x,y}(-0.5, y) - F_{x,y}(-1, y)}{F_x(-0.5) - F_x(-1)}. \quad (8)
 \end{aligned}$$

The conditional probability expectation of (8) is the possible vegetation change value.

For moderate drought, severe drought, and extreme drought categories, the most likely vegetation change value can be derived with the same procedure by changing the range of x . For AN_SPI, an accumulated SPI value, we define mild drought, moderate drought, severe drought, and extreme drought with five months of the growing season multiplied by the range of the SPI. The flowchart of the multidimensional copula joint distribution model is shown in Fig. 2. The Gaussian distribution was used for modeling vegetation variation (Var_NDVI/Var_EVI) in the series. The GEV model was used for the drought condition variable series (MIN_SPI/AN_SPI). The Archimedean copula function was chosen to develop the joint distribution of the vegetation biomass index and drought index.

IV. RESULTS AND ANALYSIS

A. Temporal and Spatial Characteristics of the SPI and NDVI/EVI in the TRH

1) *Temporal Evolution Characteristics of the SPI*: The left column of Fig. 3 shows the temporal change in the regional averaged SPI1, SPI3, SPI6, and SPI12. The right column shows the temporal change in the regional minimum SPI3 in spring, summer, autumn, and winter. The linear fitting slopes of the SPI series in the left column are 0.004, 0.005, 0.005, and 0.005, and

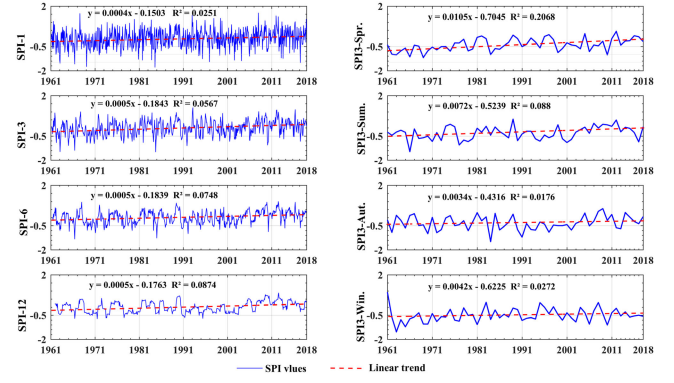


Fig. 3. Temporal characteristics of the drought in the TRH from 1961 to 2018. The left column represents the SPI on time scales 1, 3, 6, and 12 months; and the right column is the seasonal SPI in spring, summer, autumn, and winter.

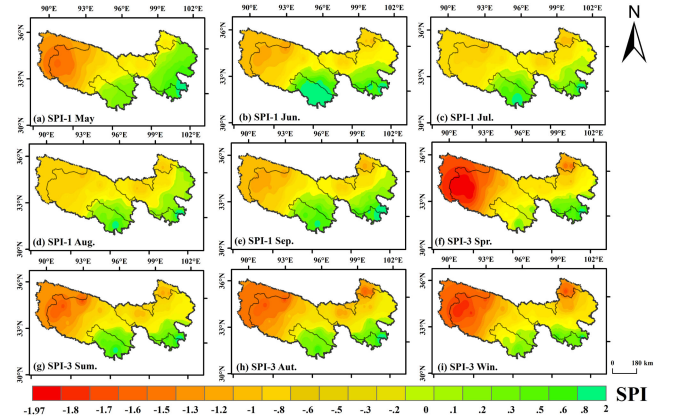


Fig. 4. Spatial distribution of the SPI in the TRH. (a)–(i) SPI1 May, SPI1 June, SPI1 July, SPI1 August, SPI1 September, SPI3 spring, SPI3 summer, SPI3 autumn, and SPI3 winter, respectively.

the R^2 values are 0.0251, 0.0567, 0.0748, and 0.0874, respectively. Monthly severe drought events (SPI1) were found in 1963, 1966, 1969, 1984, 1997, and 2017. Seasonal moderate drought (SPI3) years included 1963, 1966, 1984, 1992, 2000, and 2017. Mid-to-long-term moderate drought events (SPI6) occurred in 1966 and 1985. Annual mild drought events (SPI12) occurred in 1966, 1971, 1973, 1991, and 1995. The linear fitting slopes of the SPI series in the right column are 0.0105, 0.0072, 0.0034, and 0.0042, respectively. The R^2 values are 0.2068, 0.088, 0.0176, and 0.0272, respectively. This result means that the TRH area has gradually become wetter during the past 58 years. SPI3 in spring had the most significant increasing trend. The alternating wet and dry conditions in autumn and winter were more obvious than those in spring and summer.

2) *Spatial Distribution Characteristics of the SPI*: Inverse distance weighting (IDW), which was tested more consistently with the actual drought distribution in the TRH, was used as the interpolation method. The spatial interpolation and visualization of the SPI values were implemented in the ArcGIS program. Fig. 4 refers to the SPI spatial distribution during the 58-year period. Fig. 4(a)–(e) shows the spatial distribution of the minimum SPI1 values in May, June, July, August, and September

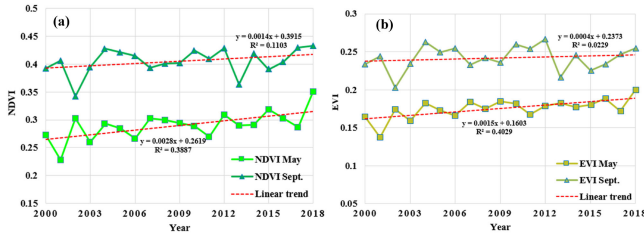


Fig. 5. Temporal evolution of the vegetation index. (a) NDVI. (b) EVI.

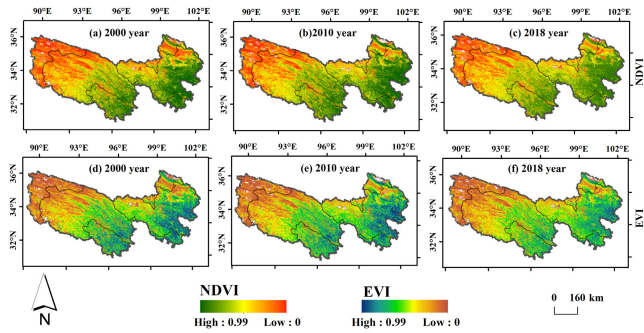


Fig. 6. Spatial and temporal distribution of the vegetation index in the TRH.

(local vegetation growing season). Fig. 4(f)–(i) shows the multi-year averaged minimum SPI3 in spring (March–May), summer (June–August), autumn (September–November), and winter (December–February). The spatial distribution of drought in the region had significant regional heterogeneity. The northwestern part of the Yangtze River suffers the greatest drought threat, followed by the northwestern part and the northeastern part of the Yellow River. The southeastern region of the TRH is relatively moist. In addition, the spatial distribution of the SPI3 in winter and spring showed a more severe drought situation.

3) *Temporal Evolution Characteristics of the NDVI/EVI*: Fig. 5 plots the temporal series of the NDVI and EVI in May and September from 2000 to 2018. This result indicated that the NDVI value was higher than the EVI, and the NDVI and EVI values in September were both higher than those in May. The linear trend slopes were all greater than 0, meaning the vegetation coverage improved in that time. In addition, the Pearson correlation coefficients of the NDVI and EVI were calculated and both were higher than 0.9, indicating that the two vegetation indices had a high degree of positive correlation.

4) *Spatial Coverage Characteristics of the NDVI/EVI*: Fig. 6 shows the spatial distribution of the vegetation index (NDVI/EVI) from 2000 to 2018 in the TRH region. The two vegetation indices have the corresponding spatial distribution characteristics: the vegetation coverage in the northwest is relatively low, and the vegetation coverage in the Lancang River and the southeast of the Yellow River is relatively high.

B. Trend Characteristics of the SPI and NDVI/EVI

1) *Trend Characteristics of the SPI*: Fig. 7 shows the trend characteristics of the SPI. A positive Z value indicates an upward

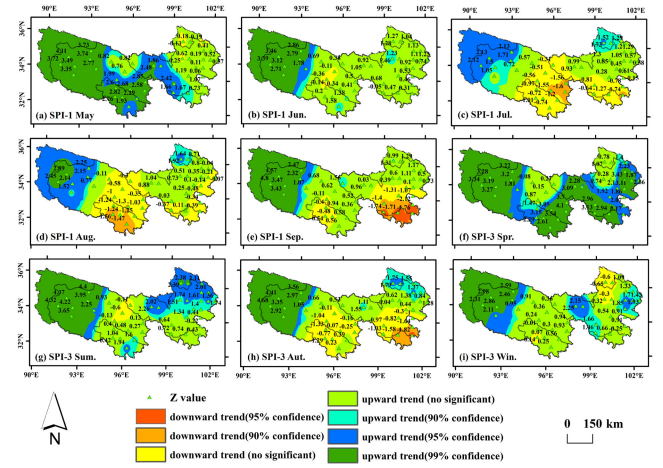


Fig. 7. Monthly and seasonal trends (Z values) of the SPI in the TRH area.

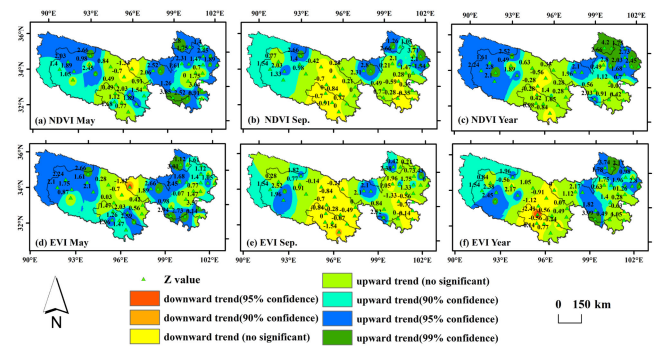


Fig. 8. Change trends (Z values) of the NDVI and EVI from 2000 to 2018.

(wet) trend in the SPI series. A negative Z value indicates a downward (drought) trend in the SPI value. When the absolute value of Z is greater than 1.28, 1.64, and 2.32, the significance tests of 90%, 95%, and 99% of confidence are passed, respectively. The regional average Z values from May to September were 1.64, 1.11, 0.26, 0.24, and 0.63, respectively. The proportions of the SPI with upward trends were 7.32%, 10%, 42.5%, 50%, and 30%. The average Z values of the four seasons were 2.28, 1.58, 0.65, and 1.03, respectively. The proportions of the SPI with upward trends were 2.5%, 10%, 42.5%, and 17.5%. This result reveals that the TRH tends to be wet overall. The most significant wet trend was found in spring, but an insignificant drought trend was found in autumn. More specifically, the northwestern region of the Yangtze River had a significant wet trend. The southeastern area of the Yangtze River had a significant drought trend in autumn.

2) *Trend Characteristics of the NDVI/EVI*: Fig. 8 refers to the Z values of the vegetation index in May and September and the annual average from 2000 to 2018. IDW spatial interpolation was used to obtain the vegetation change trend map. The average Z values of the NDVI in May, September, and annually were 1.54, 0.82, and 1.36, respectively, and those of the EVI were 1.44, 0.48, and 0.82, respectively. The vegetation index had an overall upward trend. It was found that the trend of vegetation

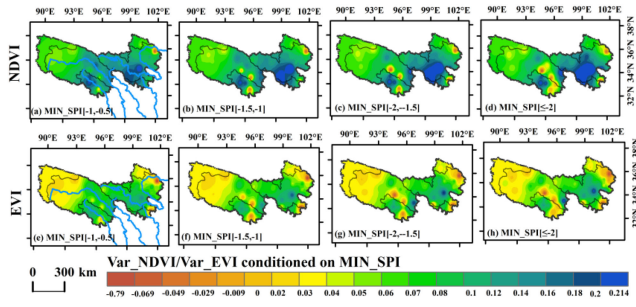


Fig. 9. Based on the spatial distribution results of the copula method combined with the NDVI/EVI and MIN_SPI3 values.

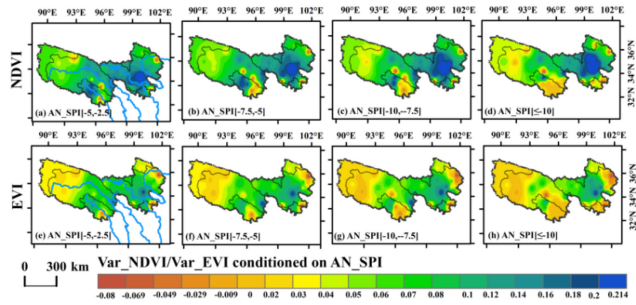


Fig. 10. Based on the spatial distribution results of the copula method combined with the NDVI/EVI and AN_SPI3 values.

change in the northern TRH area was stronger than that in the southern area and that in the west was stronger than that in the east.

C. Response of the NDVI/EVI to the SPI

1) *Response of Vegetation Growth to MIN_SPI3*: Fig. 9 shows the spatial distribution of vegetation growth under the condition of MIN_SPI3 in which there are four types of drought. Fig. 9(a)–(h) shows the conditional expectations of Var_NDVI and Var_EVI when the given SPI value is $-1 \leq \text{SPI}_3 \leq -0.5$, $-1.5 \leq \text{SPI}_3 \leq -1$, $-2 \leq \text{SPI}_3 \leq -1.5$, and $\text{SPI}_3 \geq -2$, respectively. It shows that Var_EVI is significantly more strongly affected by MIN_SPI. As severe droughts rarely occur in the TRH area, Fig. 9(c), (d), (g), and (h) provides more significant reference information. The results can be used to simulate the influence of the degree of severe drought on vegetation change.

2) *Response of Vegetation Growth to AN_SPI3*: Fig. 10 refers to the spatial distribution of the conditional expectation of vegetation growth conditioned on AN_SPI3 (accumulated negative SPI3). It was found from Fig. 10(a)–(h) that Var_EVI was significantly more affected by AN_SPI3 than Var_NDVI. Compared with Fig. 9, the vegetation growth conditioned on AN_SPI3 was more evident than that conditioned on MIN_SPI3. It can be reasonably derived that the vegetation growth caused by persistent drought events has a higher impact than that caused by extreme drought in a short time. The vegetation in the TRH area has a certain degree of drought resistance.

TABLE II
CONDITIONAL DISTRIBUTION OF THE AVERAGED NDVI IN THE GROWING SEASON REFERRING TO DIFFERENT DROUGHT DEGREES

Quantile	Kendall correlation coefficient	p value	Mild	Moderate	Severe	Extreme
q_NDVI [0.05]			0.13	0.153	0.173	0.24
q_NDVI [0.25]			0.35	0.39	0.41	0.50
q_NDVI [0.50]	0.925	0.28	0.58	0.60	0.63	0.71
q_NDVI [0.75]			0.79	0.81	0.83	0.87
q_NDVI [0.95]			0.96	0.964	0.966	0.971

TABLE III
CONDITIONAL DISTRIBUTION OF THE AVERAGED EVI IN THE GROWING SEASON REFERRING TO DIFFERENT DROUGHT DEGREES

Quantile	Kendall correlation coefficient	p value	Mild	Moderate	Severe	Extreme
q_EVI [0.05]			0.13	0.15	0.18	0.23
q_EVI [0.25]			0.36	0.39	0.41	0.48
q_EVI [0.50]	0.85	0.27	0.59	0.61	0.64	0.70
q_EVI [0.75]			0.80	0.82	0.83	0.87
q_EVI [0.95]			0.96	0.965	0.966	0.968

3) *Analysis of Conditional NDVI/EVI Distribution*: The averaged NDVI/EVI and the averaged SPI1 in the growing season of each year were extracted. The conditional distributions of averaged NDVI/EVI in each drought grade were derived. Tables II and III show the quantile values of the averaged NDVI and EVI, respectively, conditioned on different SPI grades. The first column refers to the 0.05, 0.25, 0.5, 0.75, and 0.95 quantiles. The second column is the Kendall correlation coefficient (τ) between the NDVI/EVI and SPI. The significance test p values were 0.28 and 0.27 ($p > 0.05$), respectively, meaning that the model passed the test of significance. For the 0.05 quantile, the values obtained for mild, moderate, severe, and extreme drought were 0.13, 0.153, 0.173, and 0.24, respectively. The result is reasonable because the distribution of the NDVI tends to cluster in the lower value region under severe drought. The quantile increased with increasing drought, indicating that the vegetation index was distributed increasingly toward the low values. The extreme drought had the greatest impact on vegetation, followed by severe drought and finally moderate drought. Furthermore, the positive correlation of q_NDVI was as high as 92.5%, and the q_EVI was 85%. Both results showed that the remote-sensing vegetation index was highly dependent on the drought index. This part also showed that the copula method had the potential to find the internal relationship between the NDVI/EVI and SPI.

4) *Response of Vegetation Changes to Drought Stress*: Fig. 11 shows the spatial distribution of the response value q_NDVI based on the copula method. Through spatial interpolation in the TRH region, a DNVI quantile response distribution map could be made, depicting that the NDVI decreases with

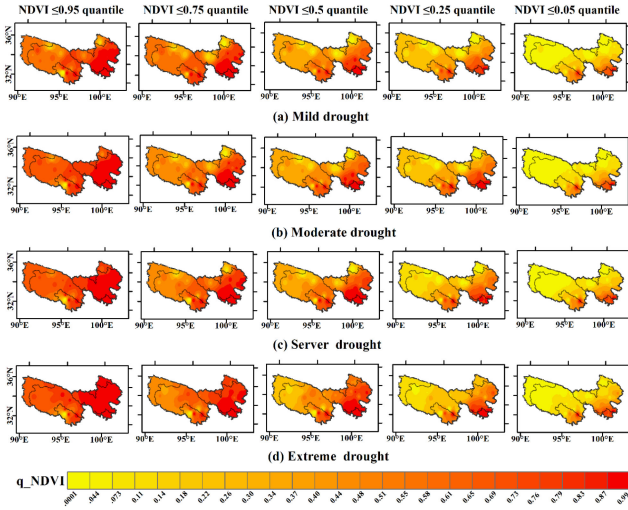


Fig. 11. Multidimensional spatial distribution of the response values of monthly NDVI to multiple drought levels under different quantiles of long-term sequences. (a)–(d) Spatial distribution of the response value q_NDVI of the SPI of the 0.05–0.95 quantiles of the NDVI, respectively.

increasing drought degree. This result means that more NDVI is lost. The study found that for the different quantiles of the vegetation index, the spatial distribution affected by the degree of the drought was different. The degree of influence of different droughts on vegetation was different. The q_NDVI value under different drought conditions had spatial variability, which was generally manifested in the Lancang River, the south of the Yangtze River, and the south of the Yellow River. There was a significant decrease in the NDVI, indicating that there was a loss of vegetation under different degrees of drought stress.

V. DISCUSSION

A. Spatiotemporal Evolution of Drought

This study was based on the SPI for drought assessment analysis. Zhang *et al.* [56] found that the SPI could respond well to drought changes. Moreover, the remote-sensing vegetation index NDVI/EVI was used to analyze the spatial and temporal evolution of vegetation. We found that the vegetation cover in the TRH area has increased since 2000, and the vegetation increase area is mainly distributed in the northwest of the Yangtze River. Additionally, some areas in the north of the Lancang River and some areas in the western part of the Yellow River have obvious vegetation degradation. Previous research produced results similar to our conclusion. Qian and Yang [57] studied the response of grassland vegetation in the TRH region to climate change, indicating that grassland vegetation had a significant improvement trend after 2004. Liu *et al.* [58] found a trend of grassland reduction during the period 1970–2004. These conclusions are consistent with the previous research conclusions of scholars. This study also found that the proportion of regions where the seasonal drought slowed in the TRH first decreased and then increased. There were vast differences in different basins, and the drought trend became evident in the summer of 2017. This

result is consistent with the research by Jinmei *et al.* [59], who noted that a drought disaster occurred in this area in July 2017.

B. This Study and Previous Studies

Hernina and Yandi [60] found that the SPI had a close relationship with the vegetation index. Previous studies focused more on the quantitative relationship between the vegetation and drought through a single correlation analysis [61]. Nevertheless, few studies are currently based on the combined distribution of regional copies and multiple NDVI scenarios to quantify the multiple responses of vegetation drought. Fang *et al.* [40] noted that the NPVI was connected to SPI based on the copula method, and the conditional probability of vegetation growth could be estimated for various drought degrees. The TRH region has a fragile environment that does not capture the vegetation-drought response. Therefore, we innovatively used the copula method to combine multiple remote-sensing vegetation indices with the SPI. Since the establishment of the TRH conservation area in 2001, the growth trend of vegetation has improved, but a decline in vegetation coverage in some areas is still apparent [62], [63]. Therefore, it is vital to explore the relationship between vegetation growth and climate factors in the region. We found that AN_SPI showed more prominent effects than Min_SPI for different drought characteristics, especially for the Lancang River and the area north of the Yangtze River. According to the combination of different aliquots of NDVI and different SPI1, the response of vegetation to drought could be evaluated from multiple angles, multiple directions, and with high precision; additionally, the vegetation cover change in the TRH area was further explored. This study found that the change in vegetation index had a higher correlation with the cumulative negative SPI value than with the quarterly minimum SPI value, indicating that continuous water shortage had a larger impact on the TRH area, and a short duration of intense drought had relatively little impact. This result means that the TRH area has inherent drought resistance. This result is consistent with the research by Zheng *et al.* [64], who reported that the vegetation in the vegetation growing season was positively correlated with the long-term drought index and that water deficiency has a cumulative effect on vegetation. This study showed that Var_EVI was significantly more affected by Min_SPI than Var_NDVI , indicating that the vegetation index EVI in the vegetation growing season was more suitable for drought stress analysis than was NDVI. This result may be because the seasonal NDVI response to drought was lagging.

Furthermore, it was shown that the response of vegetation growth dynamics to water stress in the TRH region had a seasonal lag. At the same time, this study further explored the distribution of the monthly vegetation index under multiple conditions. Meanwhile, this study did not consider other climatic factors, such as evapotranspiration, which may be helpful in more accurately measuring drought stress. This result is valuable and should be considered in future research. It is helpful to further explore the possibility of vegetation drought and the loss rate of vegetation cover caused by drought conditions in the region affected by changes in various climate elements. This

information will help us better understand the factors affecting the terrestrial ecosystem of the region and its ability to withstand such disturbances [65].

VI. CONCLUSION

This study used spatial analysis and the MK trend test method to research the spatial and temporal changes in the TRH long-term series drought index and remote-sensing vegetation index. Based on the copula multicondition joint distribution method, the multiple responses of the TRH vegetation cover change to arid climate were explored. The arid climate change over the past 58 years, the vegetation change characteristics after the 21st century, and the multiple responses of vegetation drought were discussed. The main conclusions of the study are summarized as follows.

- 1) The SPI shows that the TRH region is overall becoming more humid ($Z > 0$), but there has been an alternating drought phenomenon since the 21st century. The spatial distribution in spring and winter presented severe drought, but spring showed a significant trend of increasing humidity ($Z = 2.28$). There was a visible drought in the northwest of TRH, while the southeast was relatively humid.
- 2) Both the NDVI and the EVI had upward trends ($Z > 0$) in the TRH area that in the north was stronger than that in the south and that in the west was stronger than that in the east. The vegetation coverage in the east was significantly better than that in the northwest. The interannual NDVI showed a significant trend ($Z = 1.36$) of increasing vegetation cover.
- 3) Based on the copula combined remote-sensing vegetation index and SPI3, the EVI in the growing season was more affected by drought, and the response of vegetation to the cumulative negative SPI3 was more durable than the minimum value of SPI3, especially in the area north of the Lancang River and the Yangtze River, which also indicated that the TRH region had some drought resistance.
- 4) The monthly remote-sensing vegetation index based on the copula method showed a significant positive correlation ($p > 0.05$) with the SPI1-dependent structure, and the positive correlation coefficient of the NDVI was 0.925. There was a loss of vegetation under different degrees of drought stress in which extreme drought had the most significant impact on vegetation, while moderate drought was minimal.

REFERENCES

- [1] W. Fang, Q. Huang, S. Huang, J. Yang, E. Meng, and Y. Li, "Optimal sizing of utility-scale photovoltaic power generation complementarily operating with hydropower: A case study of the world's largest hydro-photovoltaic plant," *Energy Convers. Manage.*, vol. 136, pp. 161–172, 2017.
- [2] B. Ming, P. Liu, L. Cheng, Y. Zhou, and X. Wang, "Optimal daily generation scheduling of large hydro-photovoltaic hybrid power plants," *Energy Convers. Manage.*, vol. 171, pp. 528–540, 2018.
- [3] J. Wang, K. Wang, M. Zhang, and C. Zhang, "Impacts of climate change and human activities on vegetation cover in hilly southern China," *Ecol. Eng.*, vol. 81, pp. 451–461, 2015.
- [4] N. B. Guttman, "Comparing the palmer drought index and the standardized precipitation index," *JAWRA J. Amer. Water Resour. Assoc.*, vol. 34, pp. 113–121, 1998.
- [5] T. B. McKee, N. J. Doesken, and J. Kleist, "The relationship of drought frequency and duration to time scales," in *Proc. 8th Conf. Appl. Climatol.*, 1993, pp. 179–184.
- [6] M. Naresh Kumar, C. S. Murthy, M. V. R. Sesha Sai, and P. S. Roy, "On the use of standardized precipitation index (SPI) for drought intensity assessment," *Meteorol. Appl.*, vol. 16, pp. 381–389, 2009.
- [7] B. S. Sobral *et al.*, "Drought characterization for the state of Rio de Janeiro based on the annual SPI index: Trends, statistical tests and its relation with ENSO," *Atmos. Res.*, vol. 220, pp. 141–154, 2019.
- [8] S. Liu *et al.*, "Spatial-temporal changes in vegetation cover in a typical semi-humid and semi-arid region in China: Changing patterns, causes and implications," *Ecol. Indicators*, vol. 98, pp. 462–475, 2019.
- [9] N. Pettorelli, J. O. Vik, A. Mysterud, J.-M. Gaillard, C. J. Tucker, and N. C. Stenseth, "Using the satellite-derived NDVI to assess ecological responses to environmental change," *Trends Ecol. Evol.*, vol. 20, pp. 503–510, 2005.
- [10] J. Zhang, L. Jiang, Z. Feng, and P. Li, "Detecting effects of the recent drought on vegetation in southwestern China," *J. Resour. Ecol.*, vol. 3, pp. 43–49, 2012.
- [11] C. M. Gouveia, R. M. Trigo, S. Beguería, and S. M. Vicente-Serrano, "Drought impacts on vegetation activity in the Mediterranean region: An assessment using remote sensing data and multi-scale drought indicators," *Global Planet. Change*, vol. 151, pp. 15–27, 2017.
- [12] H.-J. Xu, X.-P. Wang, C.-Y. Zhao, and X.-M. Yang, "Diverse responses of vegetation growth to meteorological drought across climate zones and land biomes in northern China from 1981 to 2014," *Agricultural Forest Meteorol.*, vol. 262, pp. 1–13, 2018.
- [13] X. Zhang *et al.*, "Drought-induced vegetation stress in southwestern North America," *Environ. Res. Lett.*, vol. 5, 2010, Art. no. 024008.
- [14] R. K. Kaufmann *et al.*, "The effect of vegetation on surface temperature: A statistical analysis of NDVI and climate data," *Geophys. Res. Lett.*, vol. 30, 2003, Art. no. 2147.
- [15] G. Jiapaer, S. Liang, Q. Yi, and J. Liu, "Vegetation dynamics and responses to recent climate change in Xinjiang using leaf area index as an indicator," *Ecol. Indicators*, vol. 58, pp. 64–76, 2015.
- [16] F. Tian, R. Fensholt, J. Verbesselt, K. Grogan, S. Horion, and Y. Wang, "Evaluating temporal consistency of long-term global NDVI datasets for trend analysis," *Remote Sens. Environ.*, vol. 163, pp. 326–340, 2015.
- [17] R. Fensholt, K. Rasmussen, T. T. Nielsen, and C. Mbow, "Evaluation of earth observation based long term vegetation trends—Intercomparing NDVI time series trend analysis consistency of Sahel from AVHRR GIMMS, Terra MODIS and SPOT VGT data," *Remote Sens. Environ.*, vol. 113, pp. 1886–1898, 2009.
- [18] D. Dutta, A. Kundu, N. R. Patel, S. K. Saha, and A. R. Siddiqui, "Assessment of agricultural drought in Rajasthan (India) using remote sensing derived vegetation condition index (VCI) and standardized precipitation index (SPI)," *Egypt. J. Remote Sens. Space Sci.*, vol. 18, pp. 53–63, 2015.
- [19] S. Zhong, L. Di, Z. Sun, Z. Xu, and L. Guo, "Investigating the long-term spatial and temporal characteristics of vegetative drought in the contiguous United States," *IEEE J. Sel. Topics Appl. Earth Observ. Remote Sens.*, vol. 12, no. 3, pp. 836–848, Mar. 2019.
- [20] Z. Xu *et al.*, "Trends in global vegetative drought from long-term satellite remote sensing data," *IEEE J. Sel. Topics Appl. Earth Observ. Remote Sens.*, vol. 13, pp. 815–826, 2020.
- [21] F. N. Kogan, "Application of vegetation index and brightness temperature for drought detection," *Adv. Space Res.*, vol. 15, pp. 91–100, 1995.
- [22] J. Cassim and G. Juma, "Temporal analysis of drought in Mwingi sub-county of Kitui County in Kenya using the standardized precipitation index (SPI)," *Theor. Appl. Climatol.*, vol. 4, pp. 728–733, 2018.
- [23] L. Nanzad, J. Zhang, B. Tuvdendorj, M. Nabil, S. Zhang, and Y. Bai, "NDVI anomaly for drought monitoring and its correlation with climate factors over Mongolia from 2000 to 2016," *J. Arid Environ.*, vol. 164, pp. 69–77, 2019.
- [24] Y.-F. Zheng, L.-Y. Niu, R.-J. Wu, Z.-P. Wu, X.-J. Luo, and Z.-Y. Cai, "Vegetation cover change in Guizhou of Southwest China in 1982–2003 in response to climate change," *Chin. J. Ecol.*, vol. 28, pp. 1773–1778, 2009.
- [25] Y. L. Chen and Yongming, "Differences between MODIS NDVI and MODIS EVI in response to climatic factors," *J. Natural Resour.*, vol. 29, pp. 1802–1812, 2014.
- [26] L. Ji and A. J. Peters, "Assessing vegetation response to drought in the northern Great Plains using vegetation and drought indices," *Remote Sens. Environ.*, vol. 87, pp. 85–98, 2003.
- [27] D. Haro-Monteaugo, A. Daccache, and J. Knox, "Exploring the utility of drought indicators to assess climate risks to agricultural productivity in a humid climate," *Hydrol. Res.*, vol. 49, pp. 539–551, 2018.

- [28] M. Lamchin *et al.*, "Long-term trend and correlation between vegetation greenness and climate variables in Asia based on satellite data," *Sci. Total Environ.*, vol. 618, pp. 1089–1095, 2018.
- [29] Q. Lin, Z. Wu, V. P. Singh, S. H. Sadeghi, H. He, and G. Lu, "Correlation between hydrological drought, climatic factors, reservoir operation, and vegetation cover in the Xijiang Basin, South China," *J. Hydrol.*, vol. 549, pp. 512–524, 2017.
- [30] A. I. J. M. van Dijk *et al.*, "The millennium drought in southeast Australia (2001–2009): Natural and human causes and implications for water resources, ecosystems, economy, and society," *Water Resour. Res.*, vol. 49, pp. 1040–1057, 2013.
- [31] J. Peng, Z. Liu, Y. Liu, J. Wu, and Y. Han, "Trend analysis of vegetation dynamics in Qinghai–Tibet Plateau using hurst exponent," *Ecol. Indicators*, vol. 14, pp. 28–39, 2012.
- [32] S. Lawal, C. Lennard, C. Jack, P. Wolski, B. Hewitson, and B. Abiodun, "The observed and model-simulated response of southern African vegetation to drought," *Agricultural Forest Meteorol.*, vol. 279, 2019, Art. no. 107698.
- [33] L. Liang, D. Geng, T. Huang, L. Di, L. Lin, and Z. Sun, "VCI-based analysis of spatio-temporal variations of spring drought in China from 1981 to 2015," in *Proc. 8th Int. Conf. Agro-Geoinform.*, 2019, pp. 1–6.
- [34] M. Sklar, "Fonctions de repartition a dimensions et leurs marges," (in Japanese), *Publ. Inst. Statist. Univ. Paris*, vol. 8, pp. 229–231, 1959.
- [35] R. B. Nelsen, J. J. Quesada-Molina, J. A. Rodríguez-Lallena, and M. Úbeda-Flores, "Distribution functions of copulas: A class of bivariate probability integral transforms," *Statist. Probab. Lett.*, vol. 54, pp. 277–282, 2001.
- [36] L. Chen, V. P. Singh, S. Guo, A. K. Mishra, and J. Guo, "Drought analysis using copulas," *J. Hydrol. Eng.*, vol. 18, pp. 797–808, 2013.
- [37] S. Huang, B. Hou, J. Chang, Q. Huang, and Y. Chen, "Copulas-based probabilistic characterization of the combination of dry and wet conditions in the Guanzhong Plain, China," *J. Hydrol.*, vol. 519, pp. 3204–3213, 2014.
- [38] S.-C. Kao and R. S. Govindaraju, "A copula-based joint deficit index for droughts," *J. Hydrol.*, vol. 380, pp. 121–134, 2010.
- [39] K. Xu, D. Yang, X. Xu, and H. Lei, "Copula based drought frequency analysis considering the spatio-temporal variability in Southwest China," *J. Hydrol.*, vol. 527, pp. 630–640, 2015.
- [40] W. Fang *et al.*, "Probabilistic assessment of remote sensing-based terrestrial vegetation vulnerability to drought stress of the Loess Plateau in China," *Remote Sens. Environ.*, vol. 232, 2019, Art. no. 111290.
- [41] X. Wang, Y. Zhang, X. Feng, Y. Feng, Y. Xue, and N. Pan, "Analysis and application of drought characteristics based on run theory and Copula function," *Trans. Chin. Soc. Agricultural Eng.*, vol. 33, pp. 206–214, 2017.
- [42] X. Liu *et al.*, "Spatiotemporal changes in vegetation coverage and its driving factors in the three-river headwaters region during 2000–2011," *J. Geograph. Sci.*, vol. 24, pp. 288–302, 2014.
- [43] H. Cai, X. Yang, and X. Xu, "Human-induced grassland degradation/restoration in the central Tibetan Plateau: The effects of ecological protection and restoration projects," *Ecol. Eng.*, vol. 83, pp. 112–119, 2015.
- [44] X.-L. Li, G. L. W. Perry, G. Brierley, H.-Q. Sun, C.-H. Li, and G.-X. Lu, "Quantitative assessment of degradation classifications for degraded alpine meadows (Heitutan), Sanjiangyuan, western China," *Land Degradation Develop.*, vol. 25, pp. 417–427, 2014.
- [45] R. Liu, B. Lu, Y. Chen, C. Dong, X. Ruan, and W. Tang, "Analysis of arid climate characteristics of three river headwaters based on PDSI index," *Yellow River*, vol. 35, p. 59, 2013.
- [46] H. Wu *et al.*, "Grassland degradation monitoring based on changes in net primary productivity," *Pratacultural Sci.*, vol. 28, pp. 536–542, 2011.
- [47] L. Liang, L. Li, C. Liu, and L. Cuo, "Climate change in the Tibetan plateau three rivers source region: 1960–2009," *Int. J. Climatol.*, vol. 33, pp. 2900–2916, 2013.
- [48] A. Zargar, R. Sadiq, B. Naser, and F. I. Khan, "A review of drought indices," *Environ. Rev.*, vol. 19, pp. 333–349, 2011.
- [49] M. Svoboda, M. Hayes, and D. Wood, *Standardized Precipitation Index User Guide*. Geneva, Switzerland, World Meteorol. Org., 2012.
- [50] M. Gocic and S. Trajkovic, "Analysis of precipitation and drought data in Serbia over the period 1980–2010," *J. Hydrol.*, vol. 494, pp. 32–42, 2013.
- [51] H. B. Mann, "Nonparametric tests against trend," *Econometrica, J. Econometric Soc.*, vol. 13, pp. 245–259, 1945.
- [52] F. Tosunoglu and I. Can, "Application of copulas for regional bivariate frequency analysis of meteorological droughts in Turkey," *Nat. Hazards*, vol. 82, pp. 1457–1477, 2016.
- [53] K. Huang, L. Chen, J. Zhou, J. Zhang, and V. P. Singh, "Flood hydrograph coincidence analysis for mainstream and its tributaries," *J. Hydrol.*, vol. 565, pp. 341–353, 2018.
- [54] M.-T. Puth, M. Neuhäuser, and G. D. Ruxton, "Effective use of Spearman's and Kendall's correlation coefficients for association between two measured traits," *Animal Behav.*, vol. 102, pp. 77–84, 2015.
- [55] Z. Hao and V. P. Singh, "Entropy-copula method for single-site monthly streamflow simulation," *Water Resour. Res.*, vol. 48, 2012, Art. no. W06604.
- [56] Y. Zhang, J. Wang, Z. Shen, and X. Xie, "Evolution characteristics of seasonal drought in Hunan based on the standardized precipitation index (SPI)," *Geosci. Remote Sens.*, vol. 2, pp. 56–64, 2019.
- [57] S. Qian, Y. Fu, and F. PAN F, "The climate change trend and grassland vegetation response during the growing season in the Three River Source Region," *Sci. China: Earth Sci.*, vol. 40, pp. 1439–1445, 2010.
- [58] J. Liu, X. Xu, and Q. Shao, "The spatial and temporal characteristics of grassland degradation in the three-river headwaters region in Qinghai Province," *Acta Geograph. Sinica*, vol. 63, pp. 364–376, 2008.
- [59] S. Jinmei, J. Yian, Z. Yujun, and Guanqin, "Analysis of meteorological service for high temperature and drought decision-making in Qinghai Province in July 2017," *J. Qinghai Environ.*, pp. 79–83, 2018.
- [60] R. Hernina and S. Yandi, "Drought analysis by using standardized precipitation index (SPI) and normalized difference vegetation index (NDVI) at Bekasi regency in 2018," in *Proc. IOP Conf. Ser., Earth Environ. Sci.*, 2019, Paper 012002.
- [61] K. Wang, T. Li, and J. Wei, "Exploring drought conditions in the three river headwaters region from 2002 to 2011 using multiple drought indices," *Water*, vol. 11, 2019, Art. no. 190.
- [62] Z. Ying, Z. Chao-Bin, W. Zhao-Qi, Y. Yue, and L. Jian-Long, "Spatiotemporal dynamics of grassland coverage in response to climate change from 1982 to 2012 in the three rivers source region, China," *Pratacultural Sci.*, vol. 34, pp. 1977–1990, 2017.
- [63] G. Wang and G. Cheng, "Characteristics of grassland and ecological changes of vegetations in the source regions of Yangtze and Yellow rivers," *J. Desert Res.*, vol. 21, pp. 101–107, 2001.
- [64] Y. T. Zheng, Y. F. Huang, and K. Y. Wang, "Response of vegetation to water stress in the three-river headwaters region of China," *J. Basic Sci. Eng.*, vol. 26, pp. 249–262, 2018.
- [65] S. Jha, J. Das, A. Sharma, B. Hazra, and M. K. Goyal, "Probabilistic evaluation of vegetation drought likelihood and its implications to resilience across India," *Global Planet. Change*, vol. 176, pp. 23–35, 2019.



Shuang Zhu received the bachelor's degree and doctorate degree from the Huazhong University of Science and Technology, Wuhan, China, in 2012 and 2017, respectively.

Since July 2017, she has been a Lecturer and Master's Tutor with the School of Geography and Information Engineering, China University of Geosciences, Wuhan, China. Her research interests include ecological environment monitoring and early warning research based on hydrological remote sensing, deep learning, and big data technology. He currently presides over the National Natural Science Foundation Youth Fund, Central University Fund, and other projects, and participates in many national projects as a technical backbone.



Zuxiang Xiao received the bachelor's degree of science in geographic information science from Jiangxi Normal University, Nanchang, China, in 2018.

She is currently working toward the master's degree in cartography and geographic information engineering with the China University of Geosciences, Wuhan, China. Her research interests include long-term series meteorological drought assessment and geological disaster warning, and prediction research.



Xiangang Luo received the Ph.D. degree in cartography and geographic information engineering from the China University of Geosciences, Wuhan, China, in 2010.

He is currently a Doctoral Supervisor and a Visiting Scholar with the University of North Texas, Denton, TX, USA. He presided over and participated in more than 40 scientific research projects, including a number of 863 projects, major national special projects, key funds and other projects. He has authored or coauthored more than 30 papers in professional journals

at home and abroad. His main research interests include ecological environment big data, geological disaster dynamic early warning and artificial intelligence, smart water conservancy, smart city, and cloud computing.

Hairong Zhang received a doctorate degree with a major in water conservancy engineering from the Huazhong University of Science and Technology, Wuhan, China, in 2017.

He is currently with China Yangtze Power Company, Ltd., China Yichang Water Conservancy Center, and Hubei Key Laboratory of Intelligent Hydropower Science, Yangtze River Yichang Hydropower Research Institute.

Xiuwei Liu received the bachelor's degree in engineering with a major in hydrogeology and engineering geology from the Chengdu University of Technology, Chengdu, China, in 1992.

He is currently with Guiyang Geological Hazard Technical Service Center, Guiyang, China.

Rui Wang received the bachelor's degree in engineering with a major in hydrogeology and engineering geology from Guizhou University (formerly Guizhou University of Technology), Guiyang, China, in 1986.

He is currently with the Guizhou Provincial Geological Disaster Technical Service Center, Guiyang, China.

Mingzhi Zhang received the bachelor's degree with a major in information management and information systems from Beijing Forestry University, Beijing, China, in 2003.

He is currently with the Institute of Geological Environment Monitoring, China Geological Survey, Beijing, China. His main research direction is hydraulic engineering and environmental information.

Zhibin Huo received the bachelor's degree with a major in agricultural resources and environment, Hebei Agricultural University, Baoding, China, in 2003.

He is currently studying at the Institute of Hydrogeology and Environmental Geology, Chinese Academy of Geological Sciences, Beijing, China.